Mass and size dependence of single ion dynamics in molten monohalides

Olga Alcaraz and Joaquim Trullàs

Citation: The Journal of Chemical Physics **113**, 10635 (2000); doi: 10.1063/1.1323978
View online: http://dx.doi.org/10.1063/1.1323978
View Table of Contents: http://scitation.aip.org/content/aip/journal/jcp/113/23?ver=pdfcov
Published by the AIP Publishing

Mass and size dependence of single ion dynamics in molten monohalides

Olga Alcaraz and Joaquim Trullàs[a)]
Departament de Física i Enginyeria Nuclear. UPC Campus Nord, 08034 Barcelona, Spain

(Received 19 July 2000; accepted 19 September 2000)

This work is concerned with four molten monohalides with different ionic radii ratios (RbCl, NaI, AgCl, and CuCl) and ideal isotopic systems of these salts with different ionic mass ratios. The velocity autocorrelation functions of the two ionic species in each melt have been studied by both a theoretical approximation and molecular dynamics simulations. It is found that their main features may be qualitatively predicted by considering suitable combinations of the second and fourth frequency moments of their spectra. The analysis of these two parameters allows us to determine how the structure (strongly dependent on the ionic size difference) and the ionic masses contribute to the shape of the velocity autocorrelation functions. The results show that the averaged microscopic motion of the small ions is mainly determined by the first neighboring shell of unlike ions, whereas the nearest shell of like ions also affects the dynamics of the large ions. This effect is more pronounced as the size difference is greater. Furthermore, it is concluded that the size differences encourage the rattling motion of the large ions, whereas the mass difference encourages the backscattering and oscillations of the velocity autocorrelation function of the light ions. A simple rule is derived to determine the interplay between these two effects. Comparison between the mass and nearest distance ratios enables the prediction as to which species will experience a more pronounced backscattering motion. The size difference effects prevail in the hydrodynamics regime and the self-diffusion coefficient of the small ions is higher than that of the large ones. The difference between the self-diffusion coefficient increases as the size differences increases. [S0021-9606(00)50347-X]

I. INTRODUCTION

In this work, we are concerned with two classes of molten monovalent metal-ion halides: alkali halides and noble metal halides.[1–3] Alkali halides melt from a normal ionic phase and are regarded as the prototype of simple dense ionic liquids. Their structure is characterized by Coulomb ordering (alternation of the ionic species in space) and small charge penetration (first coordination shell penetration by the like charged particles). They may be realistically modeled using the Fumi–Tosi potentials.[4] These potentials are mainly characterized by the Coulomb interaction and the ionic core repulsion (which depend on two parameters, σ_+ and σ_-, related to the ionic radii). Molecular dynamics simulations (MD) proved that the velocity autocorrelation function (VACF) of the light ions is strongly oscillatory.[5] This behavior has been attributed to the ''rattling'' motion of the light ions in the relatively long-lived cage formed by its heavier neighbors of opposite charge.[6]

Copper and silver halides melt from a superionic phase or show strong premelting phenomena which result in rather large values of the ionic conductivity before melting. These systems exhibit a relatively large size difference between cations and anions; the former are smaller, more disordered, and more mobile. In an earlier work,[7] we proposed effective pair potentials for CuCl, CuBr, and CuI. These potentials, which allow for reduction in the effective ionic charges and introduce a very small ionic radii ratio ($\sigma_+/\sigma_- \approx 0.25$), are quite successful in accounting for the main structural trends observed in CuCl by neutron diffraction experiments.[8,9] While the anion–anion and cation–anion structure qualitatively resemble those of molten alkali halides, the cation–cation structure is less marked and presents a deep penetration of the cations into the first coordination shell. The nearest distances ratio found by MD is $d_+/d_- \approx 0.5$ (d_+ and d_- are the lower distances at which the $++$ and $--$ radial distribution functions are different from zero).

MD simulations of molten copper halides[10] show that, for a given melt, the self-diffusion coefficient (SDC) of the small ions (D_+) is much higher than that of the large ones (D_-), which was also experimentally observed in molten CuCl.[11] Moreover, MD shows that the VACFs of the large ions are always oscillatory while the VACFs of the small ones exhibit only a weak backscattering. Although Cu^+ are lighter than I^-, their VACFs in CuI do not present oscillations, as would be expected from molten alkali halides results. The oscillatory VACF corresponds to I^-. These results suggest that the large ions experience a rattling motion in the cage formed by the neighboring like ions while the small ones diffuse through the packed structure of slowly diffusing unlike ions.

In a later work,[12] we proposed effective pair potentials for molten AgCl and AgBr. These potentials, which also require an ionic radii ratio lower than unity ($\sigma_+/\sigma_- \approx 0.4$), provide a fair description of the available experimental total neutron scattering data.[13,14] The structural and dynamic properties of the simulated AgBr and AgCl resemble

a)Author to whom correspondence should be addressed. Electronic mail: quim.trullas@upc.es

TABLE I. Temperatures and ionic densities of the simulated salts, and the values of the parameters which do not depend on the ionic masses: the nearest distance ratio d_+/d_- [d_α is the lower distance at which $g_{\alpha\alpha}(r)\neq 0$], the partial sum rules relative to ξ_{+-} or ξ^2_{+-}, the absolute value of ξ^2_{+-} (in units of $\times 10^3$ kg^2 s^{-4}), the mean square force ratio κ_+/κ_-, and the parameter χ given by Eq. (21).

	T (K)	ρ (Å^{-3})	d_+/d_-	κ_{++}/ξ_{+-}	κ_{--}/ξ_{+-}	κ_{+-}/ξ_{+-}	κ_+/κ_-	ξ^2_{++}/ξ^2_{+-}	ξ^2_{--}/ξ^2_{+-}	ξ^2_{+-}	χ
RbCl	1023	0.0221	1.0	0.0751	0.0229	1.4045	1.0	0.1586	0.1336	2.03	1.0
NaI	1013	0.0216	0.7	0.0004	0.4454	1.2569	0.7	0.0846	0.3860	2.85	0.8
AgCl	773	0.0406	0.7	0.0082	0.7650	1.2200	0.6	0.1173	0.5900	1.60	0.7
CuCl	773	0.0443	0.5	0.0001	1.0442	0.9075	0.5	0.0415	0.6778	1.80	0.6

those obtained for NaI considering a Fumi–Tosi potential (with $\sigma_+/\sigma_-\approx 0.45$)[4] and present intermediate features between the molten alkali halides and the copper halides. In the three melts $d_+/d_-\approx 0.7$, $D_+/D_-\approx 2$, and the more oscillatory VACF corresponds to the light ions. Since in NaI the light ions are also the small ones, they will have a rattling motion in the cage formed by its heavy neighbors, as in the other alkali halides. However, the light ions in AgBr and AgCl are also the large ones. So, we cannot conclude if the oscillatory backscattering motion of Br^- and Cl^- corresponds to the caging effects with its heavy neighbors or its neighboring like ions.

The question we want to address below is how the mass and size differences contribute to the dynamics of the single ions in the above melts. In order to answer this question, we have studied by both a theoretical approximation and MD simulations the VACFs of four molten monohalides: RbCl ($d_+/d_-\approx 1$) and NaI ($d_+/d_-\approx 0.7$), as representative of alkali halides, and AgCl ($d_+/d_-\approx 0.7$) and CuCl ($d_+/d_-\approx 0.5$), as representative of noble metal halides.

In a first step, we have considered the simple theoretical approximation that Tankeshwar and Tosi[15] used to relate the difference of the SDCs for cations and anions to the liquid structure of molten copper halides. However, we have applied this approximation to calculate the VACFs and the results have been compared with those obtained by MD. Since the approximate VACFs reproduce qualitatively the main features of the VACFs obtained by MD, we have used this approximation to analyze them. The approximation characteristics each VACF by two parameters, which depend on (i) the pair potentials and the radial distribution functions, i.e., structural properties of the system, and (ii) the ionic masses. In this work we have separated the two contributions in order to analyze how the structure (strongly dependent on the difference between the size of the ionic species) and the mass contribute to the shape of the VACFs. We have tried to find a simple rule to determine the interplay between these two effects.

To gain further insight into this problem, we have also performed an ideal computer experiment of isotopic substitution. For each salt, we have carried out a series of MD simulations considering the same interionic potential but different ionic mass ratios m_+/m_-. Since the structural properties do not depend on the ionic masses, the experiment allows us to analyze, for a given liquid structure, the influence of the ionic mass difference on the characteristics of the ionic motions.

The layout of the paper is briefly as follows. The simulated systems are described in Sec. II. A theoretical approximation is developed in Sec. III. The corresponding results are discussed in Sec. IV. MD results of the isotopic systems are presented in Sec. V. Finally, in Sec. VI we give a short summary and some concluding remarks.

II. SIMULATED SYSTEMS

We have studied molten RbCl, NaI, AgCl, and CuCl, and CuCl near the melting point. The temperature T and the ionic density $\rho=(N_++N_-)/V$ for each system are indicated in Table I. We have assumed the effective pair potentials $\phi_{\alpha\beta}(r)$ of Fumi–Tosi reviewed by Sangster and Dixon[4] for RbCl and NaI, and the potentials proposed by Tasseven *et al.*[12] for AgCl and those given by Stafford *et al.*[7] for CuCl.

MD simulations of the four melts have been carried out by considering systems made up of 108 cations (N_+) and 108 anions (N_-) placed in a cubic box with periodic boundary conditions.[16] The positions and velocities of the ions have been computed using the Beeman's integration algorithm with a time step of 5×10^{-15} s. The long-range Coulomb interactions have been calculated according to the Ewald method.[4]

The evaluated properties of interest in this paper are the radial distribution functions, $g_{\alpha\beta}(r)$, and the normalized VACF

$$\psi_\alpha(t)=\frac{m_\alpha}{3k_BT}\langle \mathbf{v}_{i\alpha}(t)\cdot\mathbf{v}_{i\alpha}(0)\rangle = \frac{m_\alpha}{3k_BT}\frac{1}{N_\alpha}\sum_{i\alpha=1}^{N\alpha}\langle \mathbf{v}_{i\alpha}(t)\cdot\mathbf{v}_{i\alpha}(0)\rangle, \tag{1}$$

where m_α is the ionic mass of species $\alpha(\alpha\equiv +,-)$, k_B is the Boltzmann's constant, $\mathbf{v}_{i\alpha}(t)$ is the velocity of an ion of species α, and the angular brackets represent the ensemble average. The SDCs are given by the Green–Kubo formulas

$$D_\alpha=\frac{k_BT}{m_\alpha}\int_0^\infty \psi_\alpha(t)dt. \tag{2}$$

For each type of monohalide, we have also carried out several MD simulations of isotopic systems, i.e., considering the same interionic potentials, and therefore the same $g_{\alpha\beta}(r)$, for different ionic mass ratios. In order to have comparable time scales, we have kept the mean ionic mass $(m_++m_-)/2$ of the actual system.

III. THEORY

Various models have been proposed to compute the VACF by introducing different ansatzes and mode-coupling

approximations for the memory function.[17,18] Nevertheless, we have adopted another line of approach; the same adopted by Tankeshwar and Tosi.[15] We have assumed that the normalized VACF are given by the following simple functional form already proposed by Douglass[19]

$$\psi_\alpha(t)=\mathrm{sech}(t/\tau_\alpha)\cos(\omega_\alpha t). \tag{3}$$

With this approximation, Eq. (2) gives

$$D_\alpha=\frac{k_BT}{m_\alpha}\frac{\pi}{2}\tau_\alpha\,\mathrm{sech}(\tfrac{1}{2}\pi\omega_\alpha\tau_\alpha). \tag{4}$$

The two parameters τ_α and ω_α can be estimated upon comparing the Taylor series expansion of Eq. (3) with the exact short-time expansion of the VACF

$$\psi_\alpha(t)=1-\frac{1}{2!}\langle\omega_\alpha^2\rangle t^2+\frac{1}{4!}\langle\omega_\alpha^4\rangle t^4-\cdots, \tag{5}$$

where $\langle\omega_\alpha^2\rangle$ and $\langle\omega_\alpha^4\rangle$ are the second and fourth frequency moments of the spectrum of $\psi_\alpha(t)$, which can be related to integrals over particle distribution functions (sum rules). Since the square root of the second frequency moment is the Einstein frequency, which is usually denoted by Ω_0, we will denote $\langle\omega_\alpha^2\rangle$ by Ω_α^2. After long and tedious algebra, which implies the generalization to multicomponent systems of the more easily available sum rules in unicomponent liquids, Ω_α^2 can be written as

$$\Omega_\alpha^2=\langle\omega_\alpha^2\rangle=\frac{1}{m_\alpha}\frac{\langle F_{i\alpha}^2\rangle}{3k_BT}=\frac{1}{m_\alpha}\kappa_\alpha=\frac{1}{m_\alpha}\sum_{\beta=1}^{s}x_\beta\kappa_{\alpha\beta}, \tag{6}$$

where $\langle F_{ia}^2\rangle=3k_BT\kappa_\alpha$ is the mean square force acting on an α-type particle, $x_\beta=N_\beta/N$ ($N=\Sigma N_\alpha$) is the ionic fraction (in our case $x_+=x_-=0.5$), and $\kappa_{\alpha\beta}$ is given by the following partial sum rule

$$\kappa_{\alpha\beta}=\frac{4}{3}\pi\rho\int_0^\infty g_{\alpha\beta}(r)\left[\frac{d^2\phi_{\alpha\beta}(r)}{dr^2}+\frac{2}{r}\frac{d\phi_{\alpha\beta}}{dr}\right]r^2\,dr. \tag{7}$$

On the other hand, $\langle\omega_\alpha^4\rangle$ can be separated into two terms

$$\langle\omega_a^4\rangle=\langle\omega_\alpha^4\rangle_{(2)}+\langle\omega_\alpha^4\rangle_{(3)}, \tag{8}$$

where $\langle\omega_\alpha^4\rangle_{(2)}$ depends only on 2-particle distribution functions and can be written as

$$\langle\omega_\alpha^4\rangle_{(2)}=\frac{1}{m_\alpha^2}\xi_\alpha^2=\frac{1}{m_\alpha^2}\sum_{\beta=1}^{s}\left(x_\alpha+x_\beta\frac{m_\alpha}{m_\beta}\right)\xi_{\alpha\beta}^2, \tag{9}$$

with

$$\xi_{\alpha\beta}^2=\frac{4}{3}\pi\rho\int_0^\infty g_{\alpha\beta}(r)\left[\left(\frac{d^2\phi_{\alpha\beta}(r)}{dr^2}\right)^2+\frac{2}{r^2}\left(\frac{d\phi_{\alpha\beta}}{dr}\right)^2\right]r^2\,dr, \tag{10}$$

and $\langle\omega_\alpha^4\rangle_{(3)}$ depends on 3-particle distribution functions and can be approximate to[15]

$$\langle\omega_\alpha^4\rangle_{(3)}\approx\tfrac{1}{2}\Omega_\alpha^4. \tag{11}$$

On comparing the short-time expansion of Eq. (3) with Eq. (5), it is found that

$$\tau_\alpha^{-2}=\frac{\langle\omega_\alpha^4\rangle-\Omega_\alpha^4}{4\Omega_\alpha^2}=\frac{\kappa_\alpha}{4m_\alpha}(\theta_\alpha-1), \tag{12}$$

and

$$\omega_\alpha^2=\frac{5\Omega_\alpha^4-\langle\omega_\alpha^4\rangle}{4\Omega_\alpha^2}=\Omega_\alpha^2-\tau_\alpha^{-2}=\frac{\kappa_\alpha}{4m_\alpha}(5-\theta_\alpha), \tag{13}$$

where

$$\theta_\alpha=\frac{\langle\omega_\alpha^4\rangle}{\Omega_\alpha^4}\approx\frac{\xi_\alpha^2}{\kappa_\alpha^2}+\frac{1}{2}. \tag{14}$$

The main features of $\psi_\alpha(t)$ may be deduced from the θ_α values. As can be seen from Eqs. (3), (4), and (12)–(14), $1/\tau_\alpha=0$ if $\theta_\alpha=1$ which imply perfect crystalline behavior with $\omega_\alpha=\Omega_\alpha$ and $D_\alpha=0$. For $1<\theta_\alpha<5$ the $\psi_\alpha(t)$ takes negative values and present at least one minimum (the backscattering characteristic of liquid systems) which becomes deeper as the values of θ_α decreases. If $\theta_\alpha<3$, then $\tau_\alpha<\omega_\alpha$ and damped oscillations can be discernible. As θ_α gets lower, ω_α is much larger than τ_α (and closer to Ω_α) and more pronounced solidlike oscillations may be observed. On the other hand, for $\theta_\alpha>5$ Eqs. (3) and (4) become

$$\psi_\alpha(t)=\mathrm{sech}(t/\tau_\alpha)\cosh(|\omega_\alpha|t), \tag{15}$$

which decays monotonically as in low density fluids, and

$$D_\alpha=\frac{k_BT}{m_\alpha}\frac{\pi}{2}\tau_\alpha\,\mathrm{sec}(\tfrac{1}{2}\pi|\omega_\alpha|\tau_\alpha). \tag{16}$$

So, the qualitative shape of a VACF may be predicted easily from θ_a. In addition, the short-time expansion given by Eq. (5) shows that $1/\Omega_\alpha$ characterizes the initial decay time of the VACFs. Small values of $1/\Omega_\alpha$ imply that the VACF decays at short times faster than for larger values of $1/\Omega_\alpha$. Henceforth, despite the functional form of Eqs. (3) or (15) being determined by the parameters τ_a and ω_a, we will characterize the VACFs by θ_a and $1/\Omega_\alpha$.

In order to simplify the analysis further, we rewrite the sum rules for κ_α and ξ_α^2 of Eqs. (6) and (9) as

$$\kappa_+=\tfrac{1}{2}(\kappa_{++}+\kappa_{+-});\quad \kappa_-=\tfrac{1}{2}(\kappa_{--}+\kappa_{+-}), \tag{17}$$

and

$$\xi_+^2=\xi_{++}^2+\tfrac{1}{2}(1+f)\xi_{+-}^2;\quad \xi_-^2=\xi_{--}^2+\frac{1}{2}\left(1+\frac{1}{f}\right)\xi_{+-}^2, \tag{18}$$

where $f=m_+/m_-$. It is important to keep in mind that, among all the above parameters, only the six partial sum rules for $\kappa_{\alpha\beta}$ and $\xi_{\alpha\beta}^2$, as well as the two mean square forces $\langle F_{i\alpha}^2\rangle=3k_BT\kappa_\alpha$, are independent of the ionic masses. We note that ξ_+^2 and ξ_-^2 only depend on the masses fraction $f=m_+/m_-$. Furthermore, we point out that the electrostatic contribution to each $\kappa_{\alpha\beta}$ vanishes. Thus, only the short-range part of the potentials contribute to the calculations and the mean square force is due only to the first-neighbor shell of unlike ions and the nearest shell of like ions. Since the first-neighbor shell contribution to κ_α is the same for both cations and anions (κ_{+-}), the difference between the mean square

TABLE II. Values of the parameters θ_α, $1/\Omega_\alpha(\times 10^{-12}\,\mathrm{s})$, $\tau_\alpha(\times 10^{-12}\,\mathrm{s})$, and $\omega_\alpha(\times 10^{12}\,\mathrm{s}^{-1})$ obtained considering the mass ratio m_+/m_- of the actual systems.

	m_+/m_-	θ_+	$1/\Omega_+$	τ_+	ω_+	θ_-	$1/\Omega_-$	τ_-	ω_-
RbCl	2.41	3.9	0.065	0.077	8.0	2.2	0.043	0.080	19.7
NaI	0.18	2.2	0.034	0.061	24.8	5.6	0.068	0.064	5.5
AgCl	3.03	6.2	0.085	0.075	6.3	1.8	0.038	0.088	23.3
CuCl	1.78	7.5	0.074	0.058	10.6	2.0	0.038	0.074	22.8

forces acting on cations and anions is associated with the contributions of the nearest shell of like ions (κ_{++} and κ_{--}).

Taking into account that the initial decay time of the VACFs is determined by $1/\Omega_\alpha=(m_\alpha/\kappa_\alpha)^{1/2}$, it is easy to see that, at short times, $\psi_-(t)$ will decay faster than $\psi_+(t)$ if

$$\frac{m_+}{m_-}>\frac{\kappa_+}{\kappa_-}. \tag{19}$$

On the other hand, taking into account Eqs. (14) and (18), it is straightforward to show that the inequality $\theta_+>\theta_-$, which implies that the anions experience a more pronounced backscattering than the cations, leads to the following equivalent condition:

$$\frac{m_+}{m_-}>\chi, \tag{20}$$

where

$$\chi=\sqrt{b^2+1}-b, \tag{21}$$

with

$$b=\frac{\xi_{++}^2}{\xi_{+-}^2}+\frac{1}{2}-\frac{\kappa_+^2}{\kappa_-^2}\left(\frac{\xi_{--}^2}{\xi_{+-}^2}+\frac{1}{2}\right), \tag{22}$$

where b is a parameter solely determined by the pair potentials and the radial distribution functions (say the structure of the system). Hence, from the theoretical approximation we have deduced two structural dependent parameters, the mean square force ratio, κ_+/κ_-, and χ, which compared with m_+/m_- allow differentiation of the behavior of the two ionic species.

IV. RESULTS

The results obtained for the mass-independent parameters corresponding to the four melts are presented in Table I. In this table, we have also included the nearest distance ratio d_+/d_-, which quantifies the ionic size differences. Since the cations are smaller than the anions in the systems studied herein (except for RbCl, where the ionic sizes are almost equal), from now on we will refer to the cations and anions as the small and large ions, respectively.

From Table I we see that in the case of RbCl, κ_{++} and κ_{--} are much smaller than κ_{+-} (κ_{++}/κ_{+-} and κ_{--}/κ_{+-} are lower than 0.06). This result implies that the mean square force acting on an ion is practically reduced to the contribution of the first shell of unlike ions and its magnitude is almost the same for the cations and the anions ($\kappa_+\approx\kappa_-\approx 0.5\kappa_{+-}$). On the other hand, in the case of CuCl, the contribution of the like ions to the mean square force acting on a large ion is slightly higher than that of the unlike ions, whereas the contribution of the like ions to the mean square force acting on a small ion is negligible ($\kappa_-\approx 2\kappa_+\approx\kappa_{+-}$). This result confirms that the neighboring like ions play an important role in the behavior of the large ions in superionic-conductor melts. The results for NaI and AgCl are intermediate between those of RbCl and CuCl. The surprising almost exact correlation between the ratios d_+/d_- and κ_+/κ_- confirms that we are dealing with an ion-size effect. Moreover, the influence of the size difference in the ratios ξ_{++}^2/ξ_{+-}^2 and ξ_{--}^2/ξ_{+-}^2 is qualitatively similar to that on κ_{++}/κ_{+-} and κ_{--}/κ_{+-}. We also note that κ_{+-}/ξ_{+-} decreases with d_+/d_-.

We now turn to the study of the approximate VACFs obtained by Eqs. (3) or (15), and the corresponding values of τ_α and ω_α, reported in Table II. The plots in Fig. 1 illustrate the above mentioned relation between the shape of the VACFs and the values of the parameter θ_α given in Table II. Comparison between the theoretical VACF and MD results shows that the present approximation allows the prediction of the main qualitative features of the VACF. Thus, we are able to predict the solidlike oscillatory behavior of one of

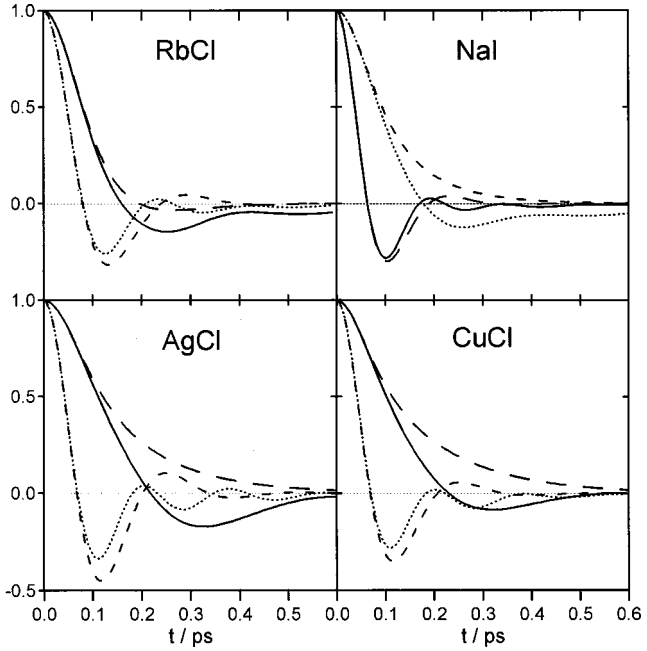

FIG. 1. Comparison between the approximate velocity autocorrelation functions obtained by Eqs. (3) or (15) (long dashed line for the cations and short dashed line for the anions) and the molecular dynamics results (solid line for the cations and dotted line for the anions).

the ionic species and the fluidlike diffusive behavior of the other. Although we use the expression fluidlike diffusive to describe a monotonically decaying (or with a weak backscattering) VACF, it does not mean that the corresponding SDC is necessarily higher than that of the other species (see the next section). In all the cases, the initial decay of VACF is well reproduced. In general, the frequency of the oscillatory theoretical VACFs is too low and the backscattering is too deep, whereas the fluidlike diffusive behavior of the other species is overestimated. We note that θ_- for NaI and θ_+ for AgCl and CuCl are higher than 5. Our results show that θ_a and $1/\Omega_\alpha$ are suitable parameters to characterize the VACFs. It is worth noting that, in these melts, the initial time decay of the solidlike oscillatory VACF is shorter than that for the other species, i.e., if θ_- is lower than θ_+, $1/\Omega_-$ is also shorter than $1/\Omega_+$. So, the main information about the shape of the VACFs is given by θ_a.

The SDCs resulting from MD show large disagreement with those obtained from Eqs. (4) or (16). Since the SDCs are k_BT/m_α times the area enclosed by $\psi_\alpha(t)$, it is obvious from Fig. 1 that the approximation used here is not a suitable approach to predict the SDCs because it does not give an accurate description of the VACFs at intermediate times. Nevertheless, we stress that the approximation is capable of describing the qualitative behavior of the VACFs and that it allows us to analyze how the mass and size differences contribute to the shape of the VACFs, as we do below.

As can be seen in Table I, the values of χ are very close to those of κ_+/κ_- and d_+/d_-. Then, the conditions given by the inequalities (19) and (20) can be reduced to the following single condition. If

$$\frac{m_{\text{small}}}{m_{\text{large}}} > \frac{d_{\text{small}}}{d_{\text{large}}}, \tag{23}$$

the VACF of the large ions will decay faster and will present a more pronounced backscattering than that of the small ones. In particular, this behavior should be observed if the mass of the large ions is equal to the mass of the small ones. Furthermore, these features will be enhanced if the large ions are lighter than the small ones, as can be corroborated in AgCl and CuCl. On the other hand, if the large ions are heavy enough the backscattering is experienced by the light ions, as in the case of NaI. Then, we could say that the size difference encourages the backscattering and oscillations of the VACF of the large ions, whereas the mass difference encourages the vibrational motion of the small ions.

V. MD OF ISOTOPIC SYSTEMS

In order to test the above conclusions, as well as to gain further insight into the mass and size difference effects, we have carried out a series of MD simulations of isotopic systems for each type of monohalide (RbCl, NaI, AgCl, and CuCl) by considering the same interionic potentials but different ionic mass ratios m_+/m_- (see Table III).

First, we will focus our attention on the isotopic RbCl systems to illustrate the mass difference effects on the averaged ionic motion. The symmetry of the $++$ and $--$ interactions (almost the same ionic sizes) in RbCl systems implies that the differences between the cation and anion motions arise solely from the mass difference. Since in these systems $d_+/d_- \approx 1$, the theoretical approximation predicts that the VACF for the light ions should be more solidlike than that for the heavy ones, as it is well suited for the actual RbCl and other molten alkali halides.[5,20] This result reveals that the light ions experience a rattling motion in the relatively long-lived cage formed by its heavier neighbors. The probability of large-angle deflections in the motions of light particles is higher than that of the heavy ions.[21] Thus, if we interchange the ionic masses in the actual RbCl ($m_+/m_- = 0.41$), the dynamics of the cations and the anions should be interchanged. In addition, if $m_+/m_- = 1$, the symmetry between the two species implies that the dynamics of cations and anions is almost identical. The VACFs obtained by MD for the isotopic systems of RbCl, plotted in Fig. 2, illustrate these mass difference effects.

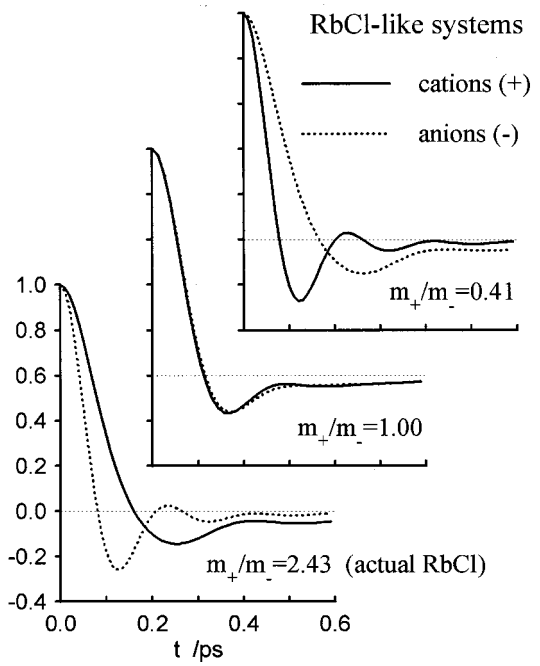

FIG. 2. The velocity autocorrelation functions obtained by molecular dynamics calculations for the RbCl-like systems (solid line for the cations and dotted line for the anions).

We now turn to study the VACFs obtained by MD simulations of the isotopic systems corresponding to NaI, AgCl, and CuCl (Figs. 3–5). Once more, it is important to keep in mind that the anions are the large ions in these systems. Comparison between the VACFs obtained for the systems with $m_+/m_- = 1$ (without mass difference effects) clearly illustrates the size difference effects on the averaged ionic motion. The theoretical approximation predicts that the large ions experience a more pronounced backscattering than the small ones in all these cases. Furthermore, the large ions VACF exhibits more solidlike oscillations, and the backscattering of the small ion VACF becomes weaker, as the size difference increases. At this point we recall that the nearest like ions contribution to the mean square force acting on a large ion becomes more important with the increase in size difference. Then, we could say that the large ions ''see''

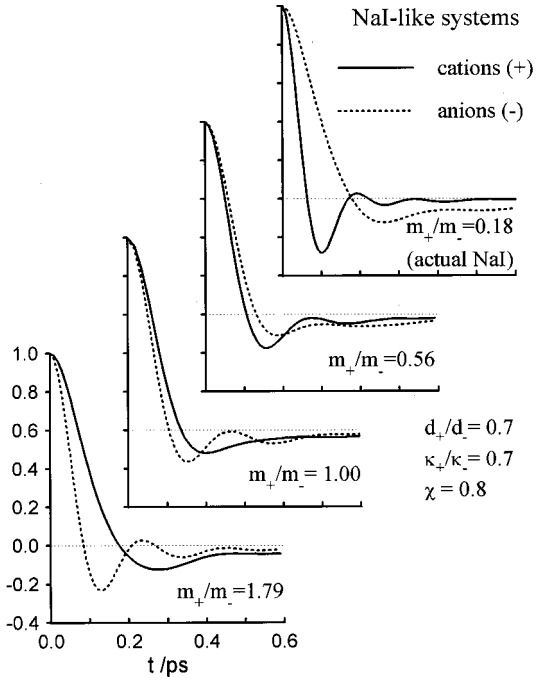

FIG. 3. The velocity autocorrelation functions obtained by molecular dynamics calculations for the NaI-like systems (solid line for the cations and dotted line for the anions).

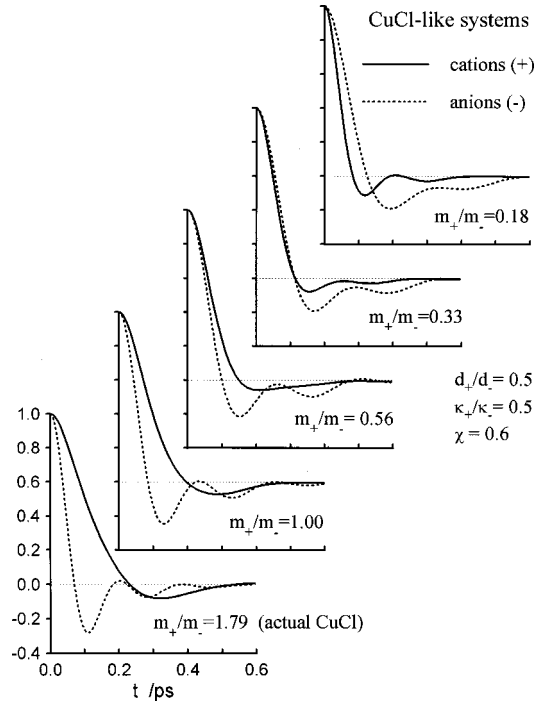

FIG. 5. The velocity autocorrelation functions obtained by molecular dynamics calculations for the CuCl-like systems (solid line for the cations and dotted line for the anions).

a double cage of small and large ions, while the small ions see only a single shell of large ions. The importance of the second shell in the double cage may be quantified by κ_{--}/κ_{+-}. Therefore, the oscillatory shape of the VACF of large ions can be pictorially interpreted as being due to the rebounds of the large ions against the surrounding double cage. On the other hand, the weaker backscattering of the small ions can be understood from the low probability of large-angle deflection in their motion inside the single shell. This simple picture for the systems with $m_+/m_-=1$ illustrates what we mean by size difference effects.

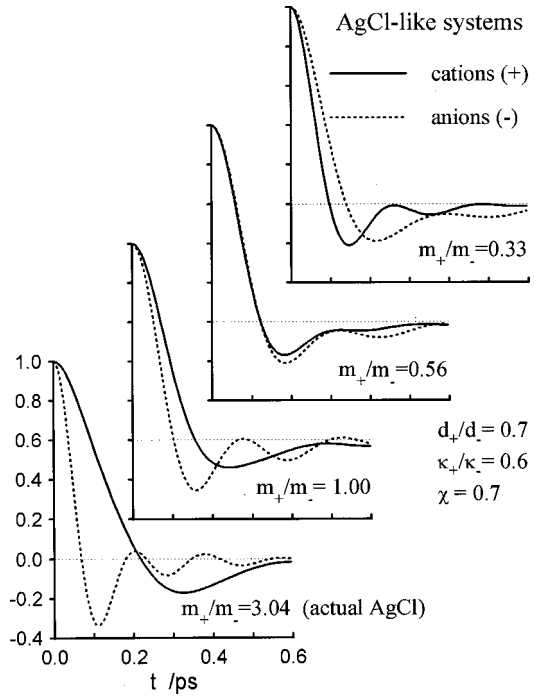

FIG. 4. The velocity autocorrelation functions obtained by molecular dynamics calculations for the AgCl-like systems (solid line for the cations and dotted line for the anions).

In Fig. 3 we show the VACFs for four NaI-like systems. Comparisons between them confirm the theoretical predictions. When $m_{\text{small}}/m_{\text{large}} > d_{\text{small}}/d_{\text{large}}$, the VACF of the large ions presents noticeable oscillations and it decays faster than that of the small ones, which shows a weaker backscattering. However, when $m_{\text{small}}/m_{\text{large}} > d_{\text{small}}/d_{\text{large}}$, the solidlike behavior corresponds to the light ions. This behavior is also observed in Fig. 4 for the AgCl-like systems. We note that for $m_{\text{small}}/m_{\text{large}}=0.56$, which is close to $d_{\text{small}}/d_{\text{large}}$, the two VACFs are very similar, as in the RbCl-like system with $m_+/m_-=1$. This suggests that the mass and size effects become compensated.

A more careful analysis is needed for the results of CuCl-like systems. Figure 5 shows that when $m_{\text{small}}/m_{\text{large}} > \kappa_{\text{small}}/\kappa_{\text{large}}$, the VACFs of the large ions decay faster than those of the small ones, and vice versa, as predicted by (19). However, the predictions about the depth of the backscattering given by (20) are not satisfied for the systems with the mass ratios equal to 0.56 and 0.18. The large ions present a more pronounced backscattering than the small ones despite of $m_{\text{small}}/m_{\text{large}} < \chi$. We could say that the size effects are more dominant than would be expected from the theoretical approximate predictions. Nevertheless, we think that the value of χ, as well as κ_+/κ_- or d_+/d_-, is quite a good measure of the size difference effects.

Finally, we comment on the SDCs obtained by MD for the isotopic systems. In the RbCl-like systems, the SDCs of

TABLE III. Values of the self-diffusion coefficient ratio D_+/D_- obtained from molecular dynamics simulations of isotopic systems as function of the mass ratio m_+/m_-.

m_+/m_-	3.0	1.8	1.0	0.56	0.33	0.18
NaI	⋯	1.4	1.5	1.6	1.7	1.8
AgCl	2.2	2.2	2.4	2.6	2.9	⋯
CuCl	⋯	3.9	4.6	5.2	6.3	7.1

cations and anions are very similar to those for the actual RbCl. In the three systems, the ratio D_+/D_- is close to 1, although the corresponding VACFs show very different behavior. The SDCs ratios for the other systems are reported in Table III. In all the cases the small ions are more diffusive than the large ones; the smaller they are, the more diffusive they become. Therefore, it is concluded that in the hydrodynamics regime the size difference effects prevail. It can be easily understood by picturing the small ions moving through the interparticle space left by the large ions. Moreover, the results of Table III show that for each set of isotopic systems the small ions are slightly more diffusive, as they are lighter.

VI. SUMMARY AND CONCLUSIONS

We have studied the velocity autocorrelation functions in molten monohalides by both a theoretical approximation and MD simulations. We have found that the main features of each VACF can be qualitatively predicted by considering suitable combinations of the second (Ω_α^2) and fourth ($\langle\omega_\alpha^4\rangle$) frequency moments of its spectra. Its initial decay time is determined by $1/\Omega_\alpha$ and its shape can be described by $\theta_\alpha = \langle\omega_\alpha^4\rangle/\Omega_\alpha^4$. As θ_α increases from 1 to higher values, the VACF changes from an oscillatory solidlike shape to a fluidlike diffusive shape. Since $1/\Omega_\alpha$ and θ_α depend on both the masses and the partial sum rules (the latter only depend on the pair potentials and the radial distribution functions), we have analyzed separately the effects of the ionic mass difference and the structure (strongly associated with the ionic size difference) on the single ion dynamics. The results show that the short-time microscopic motion of the small ions is solely determined by the first neighboring shell of large ions, whereas the dynamics of the large ions is determined by a double cage of small and large ions. The contribution of the shell of large ions to the double cage is more important when the size difference is larger.

From the overall analysis of the approximate theoretical predictions and the molecular dynamics results, we conclude that the mass difference encourages the rattling motion of the light ions, whereas the size differences encourage the oscillatory backscattering of the large ions. The mass difference effects can be measured by the mass ratio $m_{\text{small}}/m_{\text{large}}$ (m_+/m_- in the studied systems). The size difference effects can be approximately quantified by nearest distance ratio $d_{\text{small}}/d_{\text{large}}$. One of the interesting results of this work is the simple rule we have derived to predict the interplay between these two effects. When $m_{\text{small}}/m_{\text{large}} > d_{\text{small}}/d_{\text{large}}$, the large ions experience a more pronounced backscattering than the small ions. The VACFs show a more solidlike behavior as the two ratios become more different. Otherwise, the rattling motion is experienced by the light ions. Molecular dynamics simulations of isotopic systems confirm that this rule is quite satisfactory, although the size difference effect can be underestimated for systems in which the two ionic species are very different. Furthermore, the molecular dynamics results show that the size difference effects prevail in the hydrodynamics regime. Thus, the small ions are more diffusive than the large ions and the SDC of the former become higher as their ionic size decreases.

ACKNOWLEDGMENTS

We thank J. A. Padró for useful discussions and suggestions. We gratefully acknowledge the financial support of DGICYT of Spain (Grant No. PB96-0170-C03-02) and DGUR of the Generalitat of Catalonian (Grant No. 1997SGR-00149).

[1] M. P. Tosi, D. L. Price, and M. L. Saboungi, Annu. Rev. Phys. Chem. **44**, 173 (1993).
[2] M. Rovere and M. P. Tosi, Rep. Prog. Phys. **49**, 1001 (1986).
[3] J. E. Enderby and G. W. Neilson, Adv. Phys. **29**, 323 (1980).
[4] M. J. L. Sangster and M. Dixon, Adv. Phys. **25**, 247 (1976).
[5] G. Ciccotti, G. Jacucci, and I. R. McDonald, Phys. Rev. A **13**, 426 (1976).
[6] J. P. Hansen and I. R. McDonald, *Theory of Simple Liquids* (Academic, London, 1986).
[7] A. J. Stafford, M. Silbert, J. Trullàs, and A. Giró, J. Phys.: Condens. Matter **2**, 6631 (1990).
[8] I. D. Page and K. Mika, J. Phys. C **4**, 3034 (1971).
[9] S. Eisenberg, S. F. Jal, J. Dupuy, P. Chieux, and W. Knoll, Philos. Mag. A **46**, 195 (1982).
[10] J. Trullàs, A. Giró, and M. Silbert, J. Phys.: Condens. Matter **2**, 6643 (1990).
[11] J. C. Poignet and M. J. Barbier, Electrochim. Acta **26**, 1429 (1981).
[12] C. Tasseven, M. Silbert, J. Trullàs, and O. Alcaraz, J. Chem. Phys. **106**, 7286 (1997).
[13] D. A. Keen, R. L. McGreevy, W. Heyes, and K. N. Clausen, Philos. Mag. Lett. **61**, 349 (1990).
[14] M. Inui, S. Takeda, Y. Shirakawa, S. Tamaki, Y. Waseda, and Y. Yamaguchi, J. Phys. Soc. Jpn. **60**, 3025 (1991).
[15] K. Tankeshwar and M. P. Tosi, J. Phys.: Condens. Matter **3**, 7511 (1991).
[16] M. P. Allen and D. J. Tildesley, *Computer Simulation of Liquids* (Clarendon, Oxford, 1987).
[17] J. P. Boon and S. Yip, *Molecular Hydrodynamics* (McGraw-Hill, London, 1982).
[18] U. Balucani and M. Zoppi, *Dynamics of the Liquid State* (Clarendon, Oxford, 1994).
[19] D. C. Douglass, J. Chem. Phys. **35**, 81 (1961).
[20] F. Lantelme, P. Turq, and P. Schofiled, J. Chem. Phys. **67**, 3869 (1977).
[21] J. A. Padró, M. Canales, G. Sesé, and A. Giró, Physica A **148A**, 253 (1988).